Acta Crystallographica Section B
Structural Science
ISSN 0108-7681

Probability density analyses of guest ions in hollandite $A_xMg_{x/2}Ti_{8-x/2}O_{16}$ (A = K, Rb)

Yuichi Michiue

National Institute of Materials Science, 1-1 Namiki, Tsukuba, Ibaraki 305-0044, Japan

Correspondence e-mail: michiue.yuichi@nims.go.jp

Received 26 March 2007
Accepted 14 May 2007

Probability density functions (PDFs) of mobile ions in one-dimensional ionic conductors of hollandite $A_xMg_{x/2}Ti_{8-x/2}O_{16}$ (A = K, Rb) were examined by single-crystal X-ray diffraction. A conventional structure model was modified by imposing an additional constraint condition, which is based on microscopic description for the possible displacement of mobile ions adjacent to a vacancy in the tunnel. Joint PDFs and one-particle potentials for mobile ions were obtained from the structure models applying harmonic and anharmonic atomic displacement parameters (ADPs). Potential curves of the ion hopping between neighboring cavities were calculated from the joint PDF of the specific ions of the process. Energy barriers of the ion hopping were estimated at 52–60 meV from anharmonic ADP models of K-hollandite, while the values varied from 140 to 250 meV for Rb-hollandite.

1. Introduction

Structures of ionic conductors generally consist of two parts; one is the host structure and the other is the mobile ions. The former is rigid and contributes to retaining the structure of the material, while the periodicity of the latter is so disturbed in time and space by the ionic conduction. The positions of the mobile ions are rather ambiguous compared with those of the ions constructing the host structure. Thus, ion-conducting crystals are characterized by the coexistence of ordered and partially disordered structures. There are no serious problems in the structure refinements of most inorganic crystals today. Most are carried out in an established manner. However, this is not the case for ion conductors. In order to approximate the probability densities of mobile ions, two or more positions, which are close to each other, are allotted for one ion in some cases; that is the so-called 'split-atom' model. Furthermore, it is often necessary to consider the anharmonicity of the atomic displacement parameters (ADPs). As a result, parameters in least-squares refinements are strongly correlated in many cases. This problem can be partly solved by imposing the appropriate constraint conditions between parameters. For example, as the vacancy is indispensable for ion transport in crystals, the possible constraint conditions are derived by considering local structures around a vacancy. That is, a refined structure should be consistent with an assumed microscopic picture. Refinement based on such a structure model contributes to the reduction of the standard uncertainties of the parameters for the mobile ion, as recently demonstrated for sodium titanogallate (Michiue & Sato, 2004).

The hollandite structure consists of the host structure forming one-dimensional tunnels and the guest ions such as K, Rb, Cs, Ba *etc*. K-hollandite is well known as a one-dimen-

Table 1
Crystallographic data and conditions for data collection and refinement for $K_xMg_{x/2}Ti_{8-x/2}O_{16}$ ($x \simeq 1.54$) and $Rb_xMg_{x/2}Ti_{8-x/2}O_{16}$ ($x \simeq 1.51$).

Data correspond to datanames K-M23 and Rb-M24 – all refinements are given in the deposited CIF file.

	$K_xMg_{x/2}Ti_{8-x/2}O_{16}$	$Rb_xMg_{x/2}Ti_{8-x/2}O_{16}$
M_r	681.1	750.3
Space group	*I*4/*m*	*I*4/*m*
a (Å)	10.1541 (11)	10.2052 (7)
c (Å)	2.9735 (14)	2.9717 (6)
V (Å^3)	306.58 (15)	309.49 (7)
Z	1	1
D_x (g cm^{-3})	3.69	4.03
μ(Mo $K\alpha$) (mm^{-1})	5.12	10.48
Crystal size (mm)	0.25 × 0.14 × 0.14	0.15 × 0.05 × 0.05
Color	Transparent	Transparent
Radiation	Mo $K\alpha$ (0.71069 Å; graphite-monochromated)	Mo $K\alpha$ (0.71069 Å; graphite-monochromated)
Refinement of cell parameters	24 reflections ($40 \le 2\theta \le 49^\circ$)	25 reflections ($40 \le 2\theta \le 49^\circ$)
Scan mode	ω–2θ	ω–2θ
$2\theta_{max}$ (°)	100	100
Range of *h*, *k*, *l*	$-20 \le h \le 21$, $-20 \le k \le 20$, $-5 \le l \le 0$	$-21 \le h \le 21$, $-21 \le k \le 21$, $0 \le l \le 6$
Standard reflections	3 every 200	3 every 200
Reflections measured	2777	3639
Independent reflections	835	912
Observed reflections [$I_o > 3\sigma(I_o)$]	785	623
R_{int}	0.0271	0.0693
Absorption correction	Analytical	Analytical
Transmission factor	0.473–0.540	0.418–0.637
Refinement on	F^2	F^2
Weighting scheme	$1/[\sigma(I_o)^2 + 0.0001I_o^2]$	$1/[\sigma(I_o)^2 + 0.0001I_o^2]$
Extinction method	B–C type 1 Gaussian isotropic (Becker & Coppens, 1974)	B–C type 1 Gaussian isotropic (Becker & Coppens, 1974)

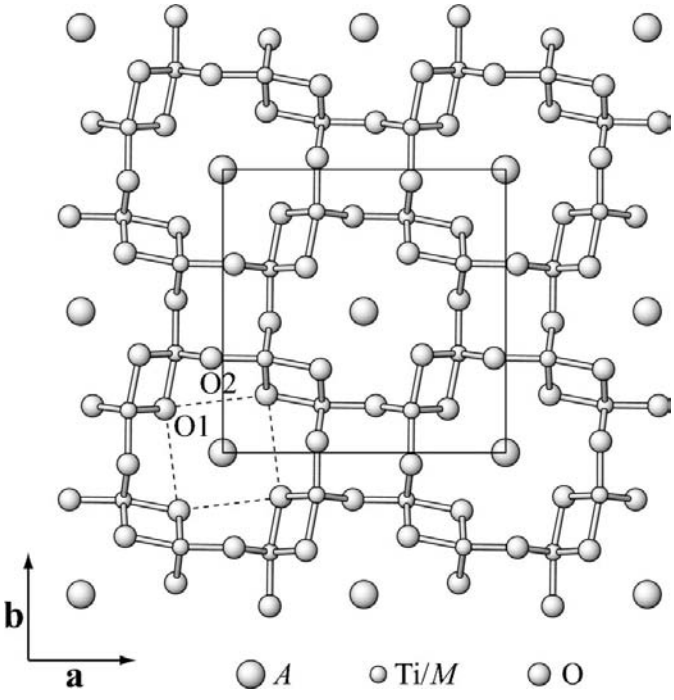

Figure 1
Structure of hollandite projected along **c**. A square of O1 ions defining the cavity is shown by dotted lines.

sional ionic conductor, in which K ions are mobile utilizing tunnels in the host structure as conduction paths (Bernasconi *et al.*, 1979; Yoshikado *et al.*, 1982). Weber & Schulz (1986) carried out refinements of hollandite $K_xMg_{x/2}Ti_{8-x/2}O_{16}$ with anharmonic ADPs. Although the structure refinement of $Rb_xAl_xTi_{8-x}O_{16}$ with harmonic ADPs was reported (Watanabe *et al.*, 1987), no anharmonic ADP model has been used for the refinement of Rb-hollandite so far. As ion transport in solids is a complicated phenomenon, careful analyses comparing various possible models are necessary. In this study structures of K- and Rb-hollandite $A_xMg_{x/2}Ti_{8-x/2}O_{16}$ (A = K, Rb) have been reinvestigated. A new type of structure model with an additional constraint condition was derived from the consideration of a possible local structure in the tunnel. Furthermore, it was examined how the results are affected by including anharmonicity in the ADPs of the mobile ion with terms up to third or fourth order. The dynamical properties of mobile ions were also discussed on the basis of the structural data. Energy barriers for the ion-hopping process were estimated by the calculation of the one-particle potential (OPP) from the joint probability density function (joint PDF) for the specific ions of the process.

2. Experimental

Single crystals of K- and Rb-hollandite were grown by the flux method. A mixture of 0.04 mol of A_2CO_3 (A = K or Rb), 0.0133 mol of MgO and 0.04 mol of TiO_2 was heated with K_2MoO_4–MoO_3 flux (0.16 mol of K_2MoO and 0.08 mol of MoO_3) at 1573 K for 20 h in a platinum crucible with a lid. The sample was cooled to 1173 K at a rate of -4 K h^{-1}, and taken out of the furnace. The flux was dissolved in hot water to separate the crystals. Crystallographic data, conditions and parameters for data collection and refinement are listed in Table 1.[1] Two types of models were used for the structure refinements. One is a conventional model used in previous works, and another is a modified model with the additional constraint condition which will be explained in §3. For each model, anharmonic atomic displacement parameters (ADPs) were considered, introducing higher-order terms (Kuhs, 1992)

[1] Supplementary data for this paper are available from the IUCr electronic archives (Reference: AV5085). Services for accessing these data are described at the back of the journal.

Table 2
Structural parameters for K ions and reliability factors for conventional and modified structure models for $K_xMg_{x/2}Ti_{8-x/2}O_{16}$.

		C(2,2)	*C*(2,3)	*M*(2,2)	*M*(2,3)
K1	*Occ*	0.19 (2)	0.38 (3)	0.297 (11)	0.310 (13)
	U^{11}	0.041 (3)	0.0284 (8)	0.0328 (10)	0.0292 (8)
	U^{33}	0.035 (5)	0.076 (15)	0.068 (4)	0.051 (4)
K2	*Occ*	0.294 (10)	0.197 (17)	0.234 (4)	0.230 (4)
	z	0.305 (5)	0.250 (8)	0.282 (3)	0.266 (4)
	U^{11}	0.0172 (4)	0.0152 (7)	0.0154 (4)	0.0164 (4)
	U^{33}	0.116 (6)	0.072 (3)	0.094 (3)	0.079 (2)
	C^{113}	–	0.0011 (8)	–	0.0020 (7)
	C^{333}	–	−0.71 (6)	–	−0.70 (6)
$R_{obs}(F)$		0.0186	0.0174	0.0189	0.0175
$wR_{obs}(F^2)$		0.0442	0.0418	0.0448	0.0419
$R_{all}(F)$		0.0203	0.0192	0.0206	0.0192
$wR_{all}(F^2)$		0.0446	0.0423	0.0452	0.0424

Fractional coordinates are $(0, 0, \frac{1}{2})$ for K1 and $(0, 0, z)$ for K2. $U^{22} = U^{11}$, $U^{12} = U^{13} = U^{23} = 0$, $C^{223} = C^{113}$, $C^{111} = C^{112} = C^{122} = C^{123} = C^{133} = C^{222} = C^{233} = 0$.

as well as harmonic ADP models. The program package *JANA*2000 (Petricek *et al.*, 2000) was used for the structure refinements and other calculations.

3. Structure models and refinement results

3.1. $K_xMg_{x/2}Ti_{8-x/2}O_{16}$

The hollandite structure consists of a host structure and guest ions (Fig. 1). In the host structure pseudocubic cavities are linearly connected to form a one-dimensional tunnel extending along **c** (Fig. 2). There are two tunnels in a unit cell; one has the center axis $(0, 0, z)$ and the other $(\frac{1}{2}, \frac{1}{2}, z)$, which are equivalent to each other because of the body-centered lattice. In order to avoid confusion, the first tunnel is used for discussion hereafter. Mobile ions are accommodated in the tunnel. In structure refinements of titania-based K-hollandite, two nonequivalent sites are primarily taken for the location of the K ions (Weber & Schulz, 1986; Watanabe *et al.*, 1987). One is the center of the cavity (0, 0, 0.5) and the other deviates from the cavity center along the tunnel direction (0, 0, *z*), where *z* ranges from 0.25 to 0.3 (approximately 0.6–0.75 Å from the cavity center). Hereafter, the former site is termed K1 and the latter is K2. As a cavity contains one K1 site and two K2 sites, the total K content per cavity is given by *Occ*[K1] + 2*Occ*[K2], which is usually less than unity. The chemical formula is generally given by $K_xM_{x/2}Ti_{8-x/2}O_{16}$ for divalent *M*. When *x* is 2, all the cavities are fully occupied by K ions. In titania-based K-hollandite, *x* is usually between 1.50 and 1.55, that is the K content per cavity varies from 0.75 to 0.775. That is, about one fourth of the cavities are vacant. When a cavity in a tunnel is vacant, the K ion in an adjacent cavity shifts toward the vacancy so as to reduce the repulsive interaction from a K ion at the opposite side, as schematically shown in Fig. 2. On the other hand, when both the adjacent sites of a K ion are occupied by other K ions, the K ion stays at the cavity center. The former corresponds to K2 and the latter corresponds to K1 in the average structure obtained from least-squares refinements. (Strictly speaking, a more detailed classification of the K sites is possible according to the environment of the K ion, as proposed by Beyeler, 1976, who considered four types of K position in a unit cell to explain the diffuse scattering of K-hollandite. However, discrimination of more than two K sites is difficult and of little use for the structure refinement.) According to this model, one vacant cavity causes two K2 ions. That is, the number of K2 ions should be twice the number of vacant cavities. As the number of K ions per unit cell is given by *m*[K1]*Occ*[K1] + *m*[K2]*Occ*[K2], the number of vacant cavities in a unit cell is given by $2 - m[\mathrm{K1}]Occ[\mathrm{K1}] - m[\mathrm{K2}]Occ[\mathrm{K2}]$, where *m*[*A*], the multiplicity of the *A* site, is 2 for the K1 site and 4 for the K2. Thus, a derived relation is

$$m[\mathrm{K2}]Occ[\mathrm{K2}] = 2(2 - m[\mathrm{K1}]Occ[\mathrm{K1}] - m[\mathrm{K2}]Occ[\mathrm{K2}]), \quad (1)$$

which has never been considered in previous works of hollandite as far I am aware, although a similar model was used for refinements of sodium titanogallate (Michiue & Sato, 2004). Note that this relation is not applicable when a K ion has vacant sites on both sides, because the K ion in that situation should stay at the cavity center and be assigned as K1. However, in the case of the present hollandites with a K (or Rb) ion concentration of more than 0.75 per cavity, configurations including a K ion with vacancies on both sides are unstable and the probability of the observation for such a local structure is so low as to be ignored, because configura-

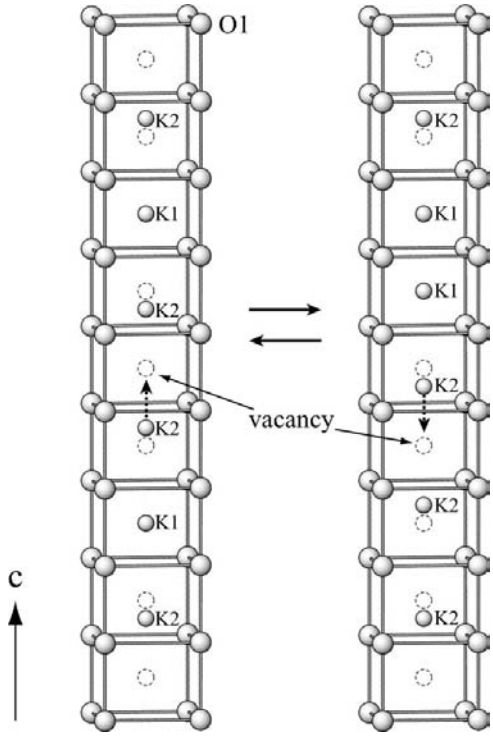

Figure 2
Schematic representations of the displacement of K ions adjacent to a vacancy.

Table 3
Structural parameters for Rb ions and reliability factors for conventional and modified structure models for $Rb_xMg_{x/2}Ti_{8-x/2}O_{16}$.

		C(2,2)	*C*(2,3)	*M*(2,2)	*M*(2,3)	*M*(2,4)
Rb1	*Occ*	0.592 (10)	0.588 (13)	0.251 (6)	0.255 (7)	0.270 (9)
	U^{11}	0.0164 (3)	0.0165 (4)	0.0184 (6)	0.0178 (8)	0.013 (2)
	U^{33}	0.188 (6)	0.182 (10)	0.032 (2)	0.028 (2)	0.044 (3)
Rb2	*Occ*	0.081 (5)	0.083 (7)	0.250 (2)	0.248 (2)	0.243 (3)
	z	0.3020 (12)	0.299 (4)	0.3266 (11)	0.3230 (19)	0.326 (3)
	U^{11}	0.0071 (8)	0.0072 (9)	0.0120 (3)	0.0123 (3)	0.0160 (15)
	U^{33}	0.012 (2)	0.013 (2)	0.0412 (11)	0.0380 (14)	0.062 (8)
	C^{113}	–	−0.0003 (7)	–	0.0002 (5)	0.0032 (19)
	C^{333}	–	−0.03 (4)	–	−0.09 (3)	0.15 (14)
	D^{1111}	–	–	–	–	0.00021 (9)
	D^{1133}	–	–	–	–	0.006 (3)
	D^{3333}	–	–	–	–	0.9 (5)
$R_{obs}(F)$		0.0222	0.0219	0.0223	0.0221	0.0218
$wR_{obs}(F^2)$		0.0418	0.0417	0.0424	0.0421	0.0416
$R_{all}(F)$		0.0605	0.0605	0.0607	0.0607	0.0603
$wR_{all}(F^2)$		0.0505	0.0504	0.0510	0.0508	0.0503

Fractional coordinates are $(0, 0, \frac{1}{2})$ for Rb1 and $(0, 0, z)$ for Rb2. $U^{22} = U^{11}$, $U^{12} = U^{13} = U^{23} = 0$, $C^{223} = C^{113}$, $C^{111} = C^{112} = C^{122} = C^{123} = C^{133} = C^{222} = C^{233} = 0$, $D^{1112} = -D^{1222}$, $D^{2222} = D^{1111}$, $D^{2233} = D^{1133}$, $D^{1113} = D^{1123} = D^{1223} = D^{1233} = D^{1333} = D^{2223} = D^{2333} = 0$. D^{1122} and D^{1112} were set to 0 because they showed no significant deviations from 0 in the refinement.

tions of K ions have a tendency to favor the separation of vacancies with nearly uniform intervals (Beyeler *et al.*, 1980; Michiue & Watanabe, 1999).

In this study, two types of models were used for the structure refinements. One is a conventional model and the other is a modified model with the additional constraint condition proposed above. Usually, two conditions were considered:

(i) full occupation at the metal site in a host structure, and

(ii) charge neutrality in a whole crystal, as given by

$$Occ[\mathrm{Mg}] + Occ[\mathrm{Ti}] = 1 \quad (2)$$

$$m[\mathrm{K1}]Occ[\mathrm{K1}] + m[\mathrm{K2}]Occ[\mathrm{K2}] = 2m[\mathrm{Mg}]Occ[\mathrm{Mg}], \quad (3)$$

where m[Mg] is 8.

That is, (2) and (3) are considered for imposing constraint conditions in the conventional model, while (1)–(3) are all satisfied in the modified model. Hereafter, conventional models are represented by *C*, and modified models with an additional constraint condition by *M*. The two numbers in parentheses following each model symbol specify the highest orders of the ADP terms for K1 and K2. [For example, model *C*(4,3) represents the conventional model with anharmonic ADP terms up to the fourth order for K1 and third order for K2, and model *M*(2,2) represents the modified model with the harmonic ADPs for both K ions.]

The structural parameters of the K ions and the reliability factors in least-squares refinements for selected models are summarized in Table 2. The introduction of fourth-order ADP terms for K2, that is the refinement for models *C*(2,4), *C*(4,4), *M*(2,4) and *M*(4,4), caused negative regions of *ca* −0.1 atom Å^{-3} in the PDF of the K2 ion. Reliability factors in these models were almost the same as those in model *C*(2,3) and *M*(2,3). Therefore, models with fourth-order ADP terms were omitted. With regard to the results in Table 2, the following should be noted:

(i) Comparing the reliability factors of harmonic ADP models, *C*(2,2) and *M*(2,2), to those of anharmonic models, *C*(2,3) and *M*(2,3), it is clear that harmonic ADPs are insufficient to describe the probability density of K ions in this hollandite.

(ii) There are almost no differences between reliability factors for *C*(2,3) and *M*(2,3), implying that the additional constraint condition does not reduce the fitting in anharmonic ADP models.

(iii) Estimated errors for most parameters in modified models are smaller than those in conventional models. It seems that parameters in conventional models are redundant and strongly correlated, while the constraint condition added in modified models contributed to reducing the correlation between parameters.

3.2. $Rb_xMg_{x/2}Ti_{8-x/2}O_{16}$

In refinements of this Rb-hollandite, two nonequivalent sites were allotted for the location of Rb ions, Rb1 $(0, 0, \frac{1}{2})$ and Rb2 $(0, 0, z)$. As was done for $K_xMg_{x/2}Ti_{8-x/2}O_{16}$, the conventional model and the modified model were examined with harmonic and anharmonic ADPs. Results for $Rb_xMg_{x/2}Ti_{8-x/2}O_{16}$ are given in Table 3, where symbols specifying the structure models are given in a similar manner to those used for $K_xMg_{x/2}Ti_{8-x/2}O_{16}$. Refinements with fourth-order ADP terms thoroughly changed the parameters giving unrealistic PDFs for Rb2 in the conventional model *C*(2,4), but yielded successful results for modified models *M*(2,4) and *M*(4,4). *M*(4,4) was omitted because reliability factors in this model were almost the same as those in *M*(2,4), despite the increase in the number of refined parameters. With regard to the results in Table 3, two points are to be noted.

(i) The improvement in refinements by introducing anharmonic ADP terms is insignificant as reliability factors for harmonic ADP models, *C*(2,2) and *M*(2,2), are close to those for anharmonic models, *C*(2,3), *M*(2,3) and *M*(2,4). However, significant changes are seen in the one-particle potential (OPP) from these models, which will be explained in §4.

(ii) The introduction of an additional constraint condition causes remarkable changes in the occupation parameters for Rb1 and Rb2, but few differences in reliability factors, as is clear by comparing the results between *C*(2,2) and *M*(2,2), or *C*(2,3) and *M*(2,3). This means that changes in the occupation parameters were compensated for by changes in other parameters such as the fractional coordinate *z* and ADPs, giving almost the same probability density for all the Rb ions from the two types of models. That is, as in $K_xMg_{x/2}Ti_{8-x/2}O_{16}$, parameters are redundant and strongly correlated in conventional models, which resulted in an alert in *PLATON* reports of conventional models of a large U_{eq} value for Rb1.

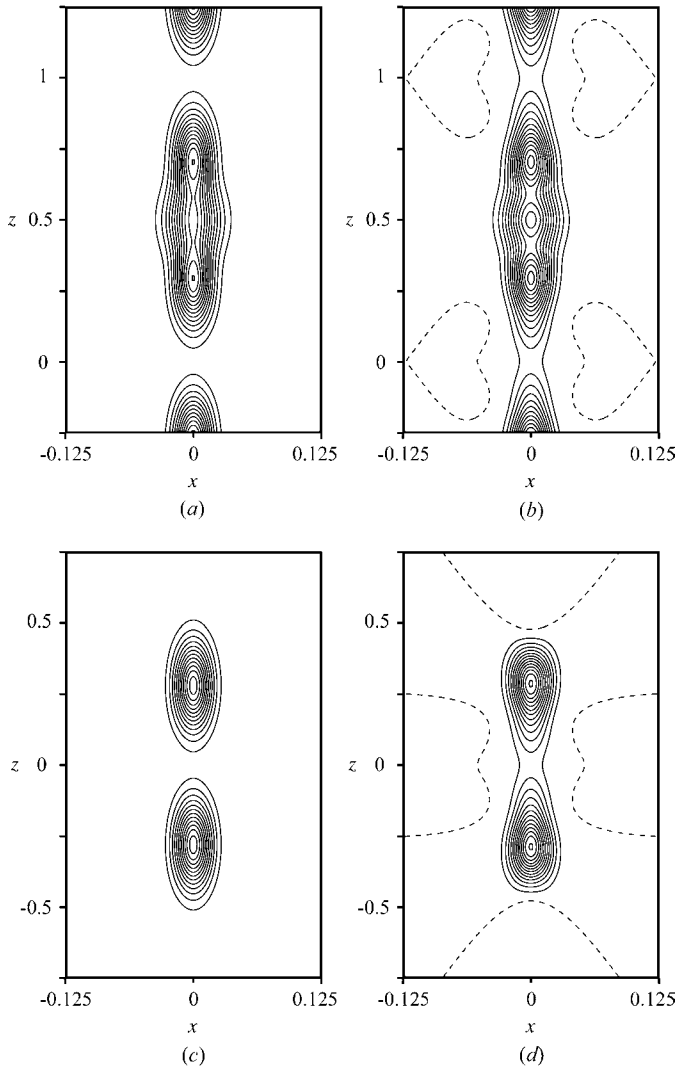

Figure 3
Joint-PDF for all K ions from model (*a*) *M*(2,2) and (*b*) *M*(2,3), and for two K2 ions in two neighboring cavities from model (*c*) *M*(2,2) and (*d*) *M*(2,3) in $K_xMg_{x/2}Ti_{8-x/2}O_{16}$. Contour intervals are 0.25 atom Å^{-3}. Broken lines are zero levels.

4. Discussion

In joint PDFs for all the K ions, density peaks corresponding to K1 at (0, 0, 0.5) and K2 at (0, 0, 0.3224) and (0, 0, 0.6776) partially overlap each other, as shown in Fig. 3(*a*) for model *M*(2,2). The density map is a little deformed by the introduction of anharmonic terms as in Fig. 3(*b*) from *M*(2,3). In a microscopic view, ion conduction in K-hollandite consists of K-ion hopping between the neighboring cavities, as schematically shown in Fig. 2. In order to consider this process, joint PDFs for only two K2 ions in the neighboring two cavities were drawn as given for *M*(2,2) (Fig. 3*c*) and *M*(2,3) (Fig. 3*d*). The densities on the (0, 0, *z*) axis were translated to an OPP as in Bachmann & Schulz (1984). Thus, the energy barrier for K-ion hopping was estimated from harmonic models to be 73 meV for *C*(2,2) and 78 meV for *M*(2,2) (Fig. 4). The values were significantly lowered in anharmonic ADP models, 52 meV for *C*(2,3) and 55 meV for *M*(2,3). Considering the insufficiency of the fitting in harmonic models, values from anharmonic ADP models are more reliable than those from harmonic ADP models. It is also noted that similar values (from 52 to 60 meV) were obtained from anharmonic ADP models with the fourth-order terms *C*(2,4), *C*(4,3), *M*(2,4) and *M*(4,3), which support the validity of the results in Fig. 4. On the other hand, in a model by Weber & Schulz (1986) anharmonic ADP terms were introduced not for K2 but K1. Instead, a small number of K ions were located at an additional site (0, 0, 0.06). Thus, a potential curve with a barrier height of ~ 30 meV was given from the joint PDF of all the K ions, although the contribution from the PDF of the K1 ion should be excluded from the calculation when considering the K-ion hopping process.

It is speculated that the K hopping between neighboring cavities is a kind of local motion which may influence properties in the microwave region. Therefore, the energy barriers given in Fig. 4 can be closely related to the conductivity at microwave frequencies. An Arrhenius plot (σT *versus* $1/T$, where σ is the conductivity) for $K_xMg_{x/2}Ti_{8-x/2}O_{16}$ at 9 GHz

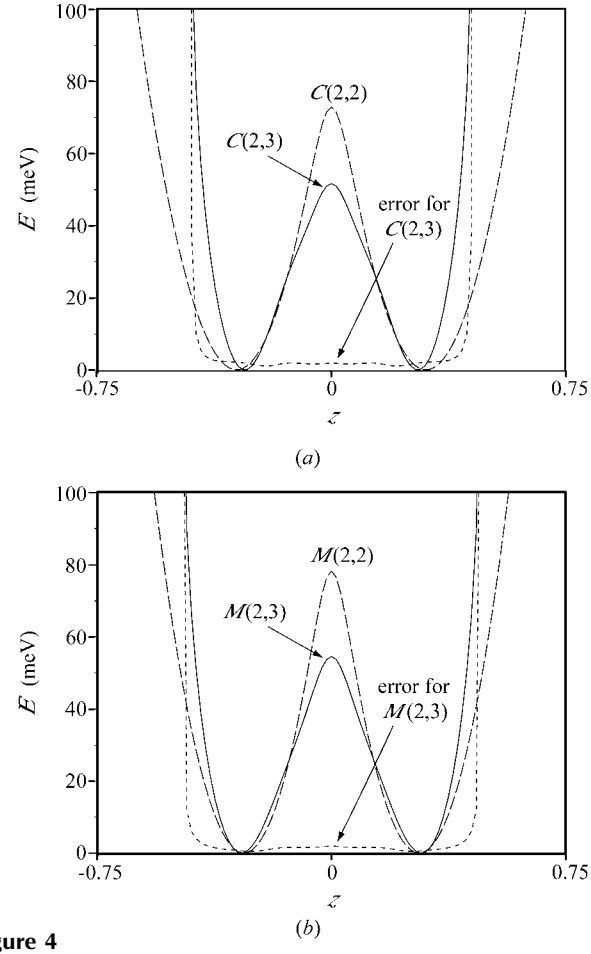

Figure 4
One-particle potentials for the K2 ion on (0, 0, *z*) from (*a*) conventional models and (*b*) modified models for $K_xMg_{x/2}Ti_{8-x/2}O_{16}$. Error curves for anharmonic models were calculated by the Monte Carlo technique.

between room temperature and *ca* 80 K showed simple thermally activated behavior with an activation energy of 34 meV (Khanna *et al.*, 1981). On the other hand, the measurement for the same hollandite at 9.54 GHz in a temperature range up to $\sim$ 500 K supported the fact that the plot significantly deviated from the line of the activation energy 34 meV at room temperature and above (Yoshikado *et al.*, 1986). Their data in the higher-temperature range are fitted by another line of activation energy roughly estimated at 80 meV. As room temperature is around the border of these two regions with different activation energies 34 and 80 meV, barrier heights of 52 and 55 meV obtained from anharmonic ADP models in Fig. 4 are consistent with the results of conductivity measurements. However, it should be noted that a Debye–Waller-type description of atomic displacement is not necessarily sufficient to explain the dynamical properties of K ions because the K–K interactions are significant, as examined by theoretical approaches based on a double chain model (Brussaard *et al.*, 2002) and atomistic simulations by the molecular dynamics method (Michiue & Watanabe, 1999). In that sense, K-hollandite is considered as a kind of incommensurate inclusion compound (van Smaalen, 1994). As ion transport in such solids is a complex phenomenon, which includes collective motion, it is also important to consider the behavior of a cluster of mobile (K) ions.

As for Rb-hollandite, an activation energy of $\sim$ 170 meV is estimated from an Arrhenius plot for the microwave conductivity of $Rb_xAl_xTi_{8-x}O_{16}$ (Yoshikado *et al.*, 1986). Joint PDFs (Fig. 5) and OPPs (Fig. 6) were also calculated using structural parameters from the models of $Rb_xMg_{x/2}Ti_{8-x/2}O_{16}$. Variations in the energy barrier for Rb-ion hopping are far more pronounced compared with those for K-ion hopping in $K_xMg_{x/2}Ti_{8-x/2}O_{16}$. The barrier heights estimated from conventional models were 790 meV for $C(2,2)$ and 670 meV for $C(2,3)$, which are far higher than that from conductivity measurements. This is mainly attributed to the low occupation factor for Rb2 in the models. In modified models the barrier height was 280 meV in the harmonic model $M(2,2)$, which was considerably reduced by the introduction of anharmonic ADP terms for Rb2, as shown in Fig. 6. The cell dimension for **a** and **b** in $Rb_xAl_xTi_{8-x}O_{16}$, 10.110 Å, is smaller than that in $Rb_xMg_{x/2}Ti_{8-x/2}O_{16}$, which caused a smaller square of O1 ions separating the cavities (see Figs. 1 and 2) in the former (diagonal length of 5.25 Å) than the latter (5.291 Å). This square of oxygen ions plays the role of a bottleneck (*i.e.* barrier) for the hopping process of the mobile ion, because the diagonal length of the square is smaller than the sum of ionic sizes of an oxygen ion (2.8 Å, twice the ionic radius of 1.4 Å) and an Rb ion (3.04 Å in six-coordination; Shannon, 1976). Considering these data, it is likely that the energy barrier in $Rb_xMg_{x/2}Ti_{8-x/2}O_{16}$ is a little lower than that in Rb_xAl_x-$Ti_{8-x}O_{16}$, 170 meV. Thus, a barrier height of 140 meV from the model $M(2,4)$ in Fig. 6 is strongly supported from crystal

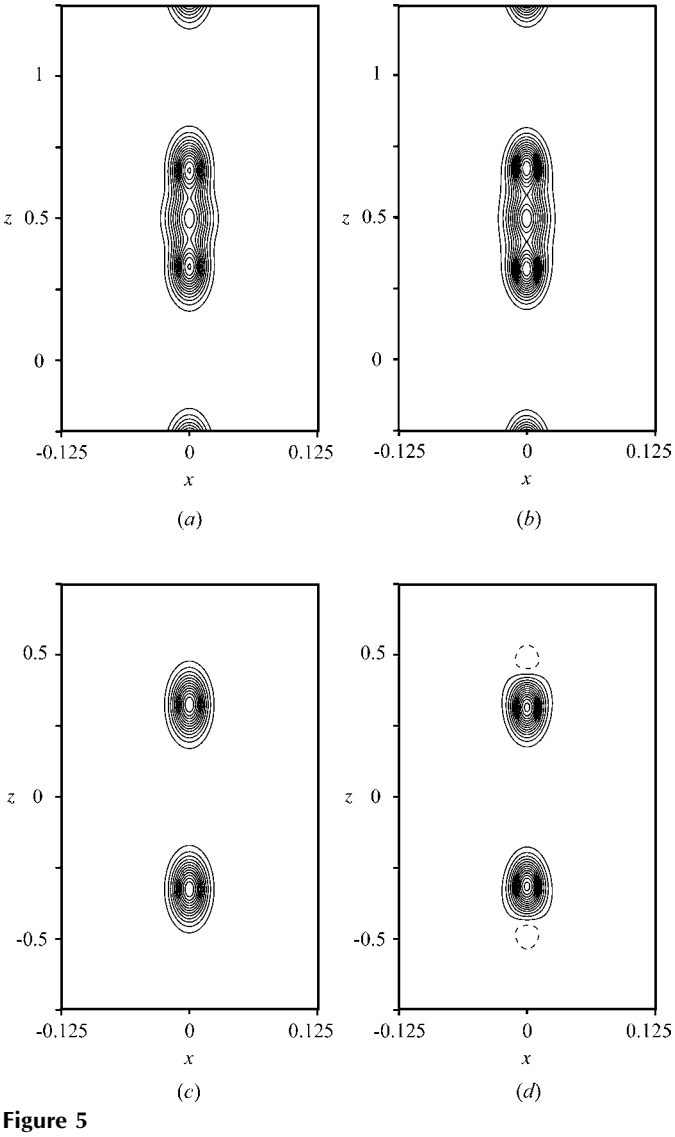

Figure 5
Joint-PDF for all Rb ions from model (*a*) $M(2,2)$ and (*b*) $M(2,4)$, and for two Rb2 ions in two neighboring cavities from model (*c*) $M(2,2)$ and (*d*) $M(2,4)$ in $Rb_xMg_{x/2}Ti_{8-x/2}O_{16}$. Contour intervals are 0.5 atom Å^{-3}. Broken lines are zero levels.

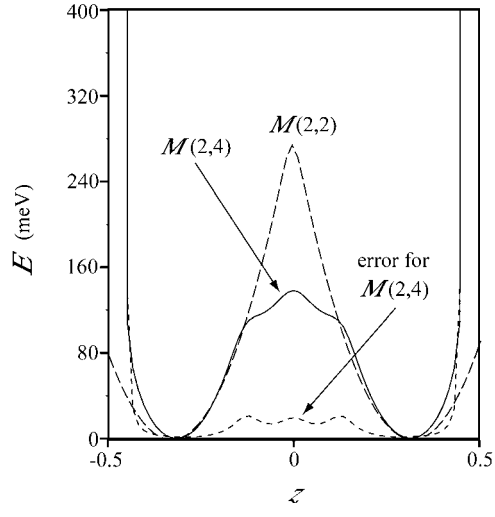

Figure 6
One-particle potentials for the Rb2 ion on (0, 0, *z*) from modified models for $Rb_xMg_{x/2}Ti_{8-x/2}O_{16}$. An error curve for $M(2,4)$ was calculated by the Monte Carlo technique.

chemical considerations. This implies that a proper structure model with anharmonic ADP terms is necessary for an accurate estimation of the energy barrier in Rb-hollandite.

The fact that the barrier height in Rb-hollandite is larger than that in K-hollandite is explained by a simple consideration based on geometrical hindrance. The diagonal length of the O1 square in $Rb_xMg_{x/2}Ti_{8-x/2}O_{16}$ mentioned above is 0.067 Å larger than that in $K_xMg_{x/2}Ti_{8-x/2}O_{16}$, 5.224 Å, while the difference between the ionic sizes of an Rb ion and a K ion is 0.28 Å in six-coordination (Rb: 3.04 Å, K: 2.76 Å) or 0.2 Å in eight-coordination (Rb: 3.22 Å, K: 3.02 Å; Shannon, 1976). Therefore, the bottlenecking effect on the hopping process is greater in $Rb_xMg_{x/2}Ti_{8-x/2}O_{16}$ than $K_xMg_{x/2}Ti_{8-x/2}O_{16}$, which causes the activation energy to be larger in the former than in the latter.

References

Bachmann, R. & Schulz, H. (1984). *Acta Cryst.* A**40**, 668–675.
Becker, P. J. & Coppens, P. (1974). *Acta Cryst.* A**30**, 129–147.
Bernasconi, J., Beyeler, H. U. & Strassler, S. (1979). *Phys. Rev. B*, **42**, 819–822.
Beyeler, H. U. (1976). *Phys. Rev. B*, **37**, 1557–1560.
Beyeler, H. U., Pietronero, L. & Strässler, S. (1980). *Phys. Rev. B*, **22**, 2988–3000.
Brussaard, L. A., Boysen, H., Fasolino, A. & Janssen, T. (2002). *Acta Cryst.* A**58**, 138–145.
Khanna, S. K., Gruner, G., Orbach, R. & Beyeler, H. U. (1981). *Phys. Rev. Lett.* **47**, 255–257.
Kuhs, W. F. (1992). *Acta Cryst.* A**48**, 80–98.
Michiue, Y. & Sato, A. (2004). *Acta Cryst.* B**60**, 692–697.
Michiue, Y. & Watanabe, M. (1999). *Phys. Rev. B*, **59**, 11298–11302.
Petricek, V., Dusek, M. & Palatinus, L. (2000). *JANA*2000. Institute of Physics, Prague, Czech Republic.
Shannon, R. D. (1976). *Acta Cryst.* A**32**, 751–767.
Smaalen, S. van (1994). *Cryst. Rev.* **4**, 79–202.
Watanabe, M., Fujiki, Y., Kanazawa, Y. & Tsukimura, K. (1987). *J. Solid State Chem.* **66**, 56–63.
Weber, H.-P. & Schulz, H. (1986). *J. Chem. Phys.* **85**, 475–484.
Yoshikado, S., Ohachi, T., Taniguchi, I., Onoda, Y., Watanabe, M. & Fujiki, Y. (1982). *Solid State Ion.* **7**, 335–344.
Yoshikado, S., Ohachi, T., Taniguchi, I., Onoda, Y., Watanabe, M. & Fujiki, Y. (1986). *Solid State Ion.* **18–19**, 507–513.